



Original article

Guaiane sesquiterpenes from seaweed *Ulva fasciata* Delile and their antibacterial propertiesKajal Chakraborty*, A.P. Lipton¹, R. Paulraj, Rekha D. Chakraborty²

Marine Biotechnology Division, Central Marine Fisheries Research Institute, Ernakulam North P.O., P.B. No. 1603, Cochin 682018, Kerala, India

ARTICLE INFO

Article history:

Received 13 December 2008

Received in revised form

24 January 2010

Accepted 25 January 2010

Available online 1 February 2010

Keywords:

Ulva fasciata Delile

Guaiane sesquiterpenoids

Antibacterial activity

Minimum inhibitory concentration

ABSTRACT

Two new guaiane sesquiterpene derivatives, guai-2-en-10 α -ol (**1**) and guai-2-en-10 α -methanol (**2**), were chromatographically purified as major constituents of the CHCl₃/CH₃OH (1:1, v/v) soluble fraction of *Ulva fasciata*. Acetylation of **2** furnished guai-2-en-10 α -methyl methanoate (**3**) with acetyl group at C₁₁ position. The structures of the compounds were elucidated using one and two-dimensional NMR and mass spectrometric analysis. Compounds **2** and **3** exhibited significant inhibition to the growth of *Vibrio parahaemolyticus* with minimum inhibitory concentrations of 25 and 35 μ g/mL, respectively. The electronegative C10 acetyl group with high polarisability (7.02×10^{-24} cm³) in **3** appeared to withdraw electron cloud from substituted cycloheptyl ring and (R)-3-methylcyclohept-1-ene moiety, thus acting as the nucleophilic center of the molecule resulting in high bioactivity.

© 2010 Elsevier Masson SAS. All rights reserved.

1. Introduction

Ulva fasciata Delile (Division: Chlorophycota; Class: Ulvophyceae; Order: Ulvales) belonging to the family Ulvaceae is an abundantly growing green seaweed in coastal seashore of South India. It is well known that the pathogenic microbes in the oceanic ecosystem can devastate populations of seaweeds. Yet, these sessile organisms suffer remarkably low levels of microbial infection, despite lacking cell-based immune systems. Seaweeds use targeted antimicrobial chemical defense strategies by eliciting secondary metabolites, which are important in ecological interactions between marine macroorganisms and microorganisms [1]. Therefore, seaweeds could be a promising source of novel bioactive compounds that can help plant survival by offering protection against stress imposed by the environment. Chemical investigations of several species belonging to green seaweeds were reported to yield bioactive diterpenes, sesquiterpenes, and related compounds as the major constituents of their aerial parts [2–8].

In recent years, multiple resistances in fish pathogenic microorganisms have developed due to the indiscriminate use of commercial antibiotics that have forced into looking for new

antimicrobial substances from various natural sources like seaweeds [9,10]. Preliminary antibacterial activity of *Ulva fasciata* Delile in our laboratory justifies the logistic need to continue the investigation of various secondary metabolites from this green alga responsible for antimicrobial activity [11]. The present study was, therefore, focused on antibacterial activity directed isolation of various antimicrobial fractions from this seaweed collected near Vizhinjam harbor of Kerala, a state situated in the southwestern coast of India. The CHCl₃/MeOH (1:1, v/v) soluble fraction of *Ulva fasciata* was purified to furnish two guaiane sesquiterpene derivatives, viz., guai-2-en-10 α -ol (**1**) and guai-2-en-10 α -methanol (**2**). The latter has been acetylated to furnish guai-2-en-10 α -methyl methanoate (**3**). The compounds were characterized by different spectroscopic analysis. These compounds were evaluated for their potential antimicrobial properties against marine aquacultural pathogens, *Vibrio parahaemolyticus* MTCC 451, *V. alginolyticus* MTCC 4439, and *V. vulnificus* MTCC 1145. This report also describes the structure–bioactivity correlation analyses of the sesquiterpenoids to observe the variability in the substitution pattern of molecules and their effect on antibacterial activity.

2. Results and discussion

Guai-2-en-10 α -ol (**1**, Fig. 1) was isolated as yellowish oily liquid upon chromatography over neutral alumina columns. The IR absorption band at 2962 cm⁻¹ is due to –CH stretching vibrations. The –OH group in the skeleton exhibit free –OH stretching vibrations near 3040 cm⁻¹. Its mass spectrum exhibited a molecular ion peak at

* Corresponding author. Tel.: +91 484 2394867; fax: +91 0484 2394909.

E-mail address: kajal_cmfri@yahoo.com (K. Chakraborty).¹ Vizhinjam Research Centre of CMFRI, P.B. No. 9, Vizhinjam P.O., Thiruvananthapuram 692521, Kerala.² Crustacean Fisheries Division, Central Marine Fisheries Research Institute, Ernakulam North P.O., P.B. No. 1603, Cochin 682018, Kerala, India.

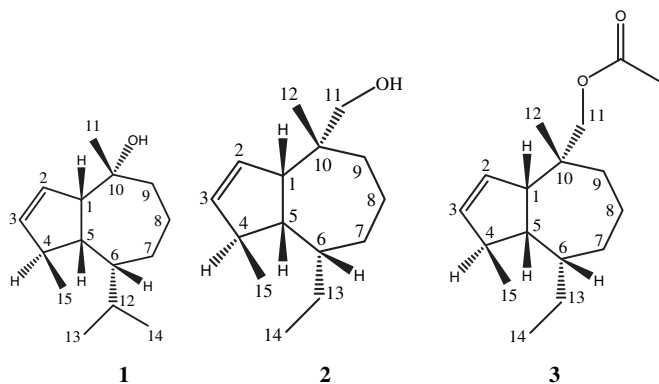


Fig. 1. Structural variations of sesquiterpenoids isolated from *Ulva fasciata*. **1:** Guai-2-en-10 α -ol; **2:** Guai-2-en-10 α -methanol; **3:** Monoacetylated derivative of **2** (Guai-2-en-10 α -methyl methanoate).

m/z 222, which in combination with its ^1H and ^{13}C NMR data (Table 1) indicated the elemental composition of $\text{C}_{15}\text{H}_{26}\text{O}$, a guaiane sesquiterpenoid hydrocarbon with three degrees of unsaturation (Fig. 1). The fragment peaks at m/z 208.3860 ($\text{C}_{15}\text{H}_{28}$) in the mass spectrum indicated the presence of decahydro-8-isopropyl-1,4-dimethylazulene, which undergoes dehydration ($-\text{H}_2\text{O}$) to afford octahydro-1,4,8-trimethylazulene ($m/z = 178.3165$). The latter fragment appeared to undergo olefinic rearrangement to afford fragment (but-2-enyl)-1,4-dimethylcycloheptane ($m/z = 180.3325$), which undergoes McLafferty rearrangement to furnish fragment ion at $m/z = 124.2256$ (3,7-dimethylcyclohept-1-ene) with the elimination of but-1-ene ($m/z = 56$, C_4H_8) (Fig. 2). The fragment ion at $m/z = 124.2256$ apparently undergoes proton elimination to yield $m/z = 122.2095$, appeared to be as 2,5-dimethylcyclohepta-1,3-diene. Cleavage of $\text{C}_1\text{-C}_7$ bond of 3,7-dimethylcyclohept-1-ene ($m/z = 124.2254$) result an ion radical (5-methyloct-3-ene) at

Table 1
NMR spectroscopic data of guai-2-en-10 α -ol (**1**) in CDCl_3 .^a

Carbon No.	$\delta^{13}\text{C}$ NMR (DEPT)	H	$\delta^1\text{H}$ NMR (int., mult., J in Hz) ^b	$^1\text{H}\text{-}^1\text{H}$ COSY	HMBC (H-C)
1	48.4 (CH)	–	–	–	–
	–	1 β	2.16 (<i>m</i>)	H-2	C-1, 5, 11
2	132.9 (CH)	2H	5.52 (<i>m</i>)	H-1	C-2
	–	–	–	–	–
3	134.5 (CH)	3H	5.34 (<i>m</i>)	H-4	C-3, 4
	–	–	–	–	–
4	44.7 (CH)	4 α	3.18 (<i>m</i>)	H-3, 5	C-4, 15
5	36.6 (CH)	5 β	1.96 (<i>ddd</i> , $J = 7.0$, 7.5, 6.8 Hz)	H-4	C-1, 5
	–	–	–	–	–
6	40.8 (CH)	–	–	–	–
	–	6 β	1.48 (<i>d</i> , $J = 7.0$ Hz)	H-7	C-6, 7, 8
7	30.9 (CH_2)	7 α	1.20 (<i>m</i>)	H-6, 8	C-8
	–	7 β	1.33 (<i>t</i> , $J = 1.8$, 1.5 Hz)	–	–
8	18.8 (CH_2)	8 α	1.24 (<i>m</i>)	H-7, 9	C-9, 11
	–	8 β	1.39 (<i>t</i> , $J = 1.5$ Hz)	–	–
9	38.2 (CH_2)	9 α	1.28 (<i>t</i> , $J = 4.8$, 2.3 Hz)	H-8	C-8
	–	9 β	1.57 (<i>m</i>)	–	–
10	73.4 (C)	10 α -OH	3.06 (<i>bs</i>)	–	C-9, 11
11	26.3 (CH_3)	CH_3 -11	2.24 (<i>s</i>)	–	C-10
12	33.5 (CH)	H-12	1.14 (<i>m</i>)	–	C-6, 13, 14
13	20.3 (CH_3)	CH_3 -13	1.06 (<i>d</i> , $J = 6.5$ Hz)	–	C-14
14	21.6 (CH_3)	CH_3 -14	1.09 (<i>d</i> , $J = 6.5$ Hz)	–	C-13
15	19.5 (CH_3)	CH_3 -15	1.17 (<i>d</i> , $J = 6.8$ Hz)	–	C-4

^a NMR spectra recorded using Bruker DPX 300 and AVANCE 300 MHz spectrometers.

^b Values in ppm, multiplicity and coupling constants ($J = \text{Hz}$) are indicated in parentheses. Assignments were made with the aid of the $^1\text{H}\text{-}^1\text{H}$ COSY, HMQC, and HMBC experiments.

$m/z = 126.2412$, which undergo further bond rearrangement to afford a conjugated ring structure (2-methylhexa-1,3-diene, $m/z = 96.1718$). Elimination of a proton and bond rearrangement in decahydro-1,4,8-trimethylazulene ($m/z = 180.3326$) leads to 1-allyl-5-methylcyclopent-1-ene with the concurrent elimination of ethylene molecule. The base peak was attributed to be due to 2,5-dimethylcyclohepta-1,3-diene ($m/z = 122.2096$) (Fig. 2). The ^1H NMR recorded four methyl signals (δ H 2.24 (*s*), 1.06 (*d*), 1.09 (*d*), and 1.17 (*d*) due to CH_3 -11, CH_3 -13, CH_3 -14, and CH_3 -15), methylenes at C-7 (δ $\text{H}_\alpha = 1.20$, δ $\text{H}_\beta = 1.33$), C-8 (δ $\text{H}_\alpha = 1.24$, δ $\text{H}_\beta = 1.39$), C-9 (δ $\text{H}_\alpha = 1.28$, δ $\text{H}_\beta = 1.57$), and methine multiplets (Table 1). The ^{13}C NMR spectrum of **1** in combination with DEPT experiments indicated the occurrence of 15 carbon atoms in the molecule including two olefinic carbons at δ 132.9 (CH) and δ 134.5 (CH), and four methyl groups (Table 1). In the $^1\text{H}\text{-}^1\text{H}$ COSY spectrum of **1**, couplings were apparent between H-1/H-2; H-4/H-3, 5; and H-3/H-4, which support the presence of cyclopentene skeleton. Also, the $^1\text{H}\text{-}^1\text{H}$ COSY correlations between H-6/H-7/H-8/H-9 supports the cycloheptane skeleton. The proton and carbon connectivities deduced from HSQC and HMBC experiments confirmed the planar framework of **1** [12]. The H-H and C-H connectivities apparent in the $^1\text{H}\text{-}^1\text{H}$ COSY and HMBC spectra respectively indicate that one of the three unsaturations in **1** was due to the double bond, and the others were due to two rings (Fig. 3). In the HMBC spectrum, it was observed that H-12/C-4, 6, 13; H₃-11/C-10; H-5/C-1, 5; and H-4/C-4, 15 were correlated with each other (Table 1). In addition, a methine proton (H-2) was coupled to the olefinic tertiary carbon (C-2) and methine H-3 with C-3. This indicated that these protons (H-2 and H-3) were connected to the olefinic tertiary carbon atoms (Fig. 3). The three degrees of unsaturation and the IR, ^1H and ^{13}C NMR spectra suggested that **1** is a bicyclic sesquiterpene with a tertiary hydroxyl group (Table 1). The FT-IR spectrum of **1** showed the absorption band for a hydroxyl group at 3040 cm^{-1} . The ^1H NMR spectrum showed an exchangeable hydroxyl proton at δ 3.06 (1H, *bs* in CDCl_3), which disappeared upon addition of D_2O . The ^{13}C NMR (Table 1) and DEPT spectra of **1** also displayed one quaternary carbon (δ 73.4) bearing a tertiary hydroxyl group. The low field quaternary signal (DEPT) at δ 73.4 is in agreement with that to a quaternary carbon signal carrying a hydroxyl group. This was supported by the relatively downfield shift of the H₃-11 signal (δ 2.24, *s*) and methine multiplet at C-1 (δ 2.16, *m*), which referred to a possible oxygenation in its vicinity. Hence, **1** is substituted at C-10 with either a α - or β -oriented hydroxyl group. The position of the hydroxyl group at C-10 was further confirmed from the $^1\text{H}\text{-}^1\text{H}$ COSY, HSQC, HMBC, and HMBC spectra. The protons at δ 1.28 (*t*, $J = 4.8$, 2.3 Hz) and δ 1.57 (*m*) exhibited a downfield shift as shown in the $^1\text{H}\text{-}^1\text{H}$ COSY NMR spectrum, and represent the methylene protons at C-9 in the neighborhood of a hydroxyl group. In a subsequent HMBC analysis the carbon at δ 73.4, bearing the hydroxyl group, correlated with a secondary methyl proton δ 2.24 (H₃-11), which showed a NOE with the protons of the cycloheptane ring (Fig. 3). The relative stereochemistry of the chiral centres of **1**, particularly that of C-10 carrying the hydroxyl group, was deduced from the NOESY spectrum of the compound and the J -values. Couplings were observed between H $_{\alpha}$ -4/H $_{\alpha}$ -7 and H $_{\alpha}$ -4/*i*Pr thus indicating that these groups must be equatorial and on the α -side of the molecule (Fig. 3). NOE correlations between H $_{\beta}$ -8/H₃-11, H $_{\beta}$ -8/H $_{\beta}$ -1, H-2/H₃-15, and H-2/H₃-11, indicated the close proximity of these groups and their β -disposition. Therefore, the C-11 methyl group is axial and β -oriented. The methyl group at C-4 group has NOE interactions with H-1, H-5, and H-6, and one of the methylene protons at C-7, which is at the β -face of the molecule (Fig. 3). A NOE correlation between CH_3 -14 and one proton on each of the carbons C-8 and C-1 was apparent; hence these are located on the β -face of the molecule and axial in configuration. The isopropyl group at C-6 is at the α -face of the molecule as it

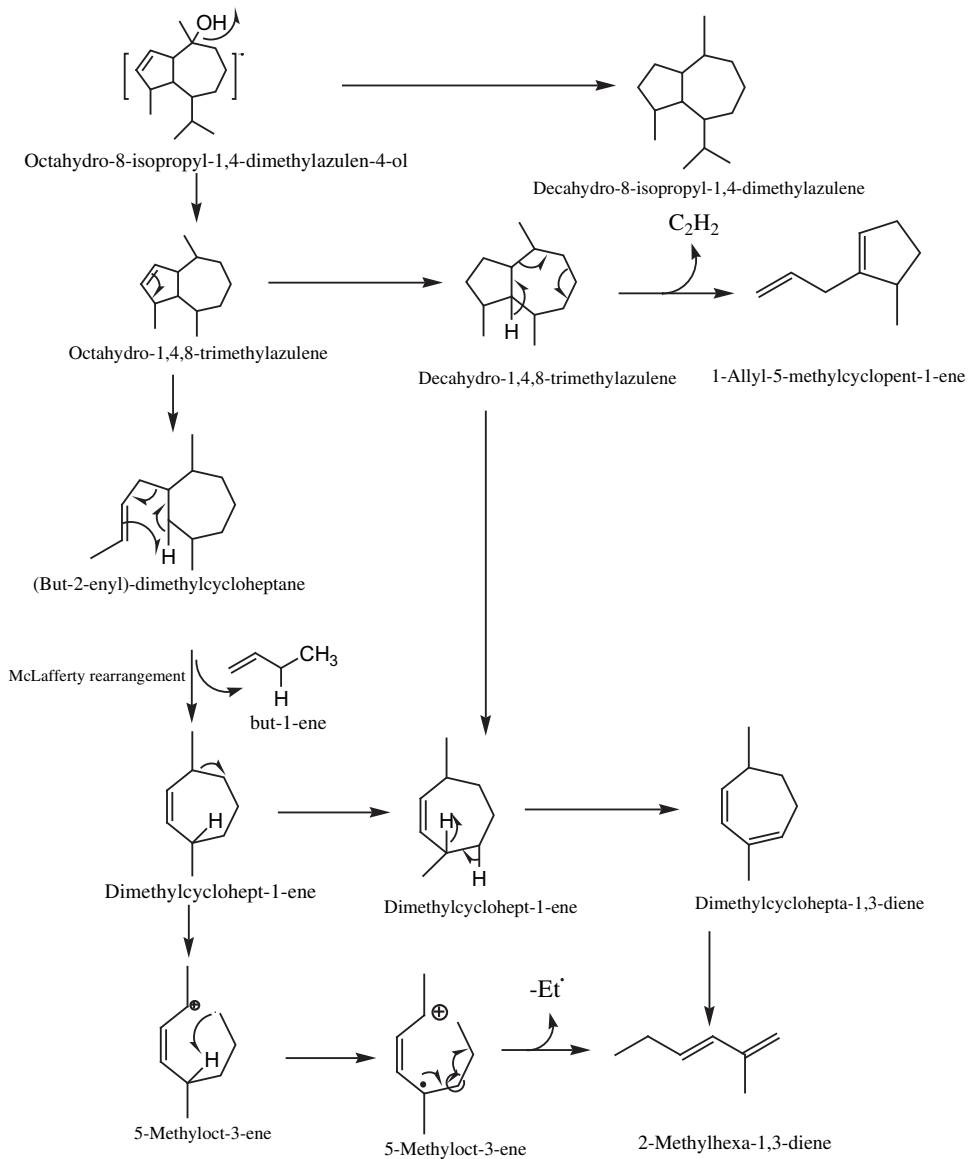


Fig. 2. Mass fragmentation pattern of guai-2-en-10 α -ol (1).

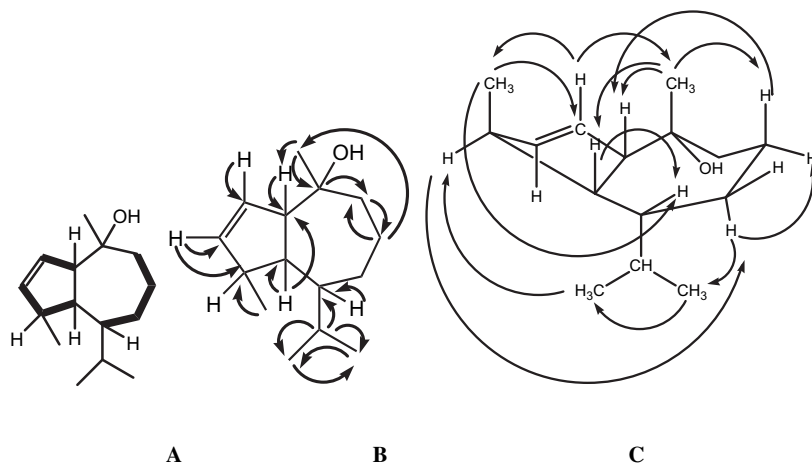


Fig. 3. 2D NMR correlations as observed in guai-2-en-10 α -ol (1). A: Key 1H - 1H COSY couplings (bold face bonds); B: HMBC couplings; C: Key NOESY correlations (long range H-H couplings are indicated as double barbed arrow).

exhibited mutual NOE interaction with H-4, and one of the protons at C-7 and C-8. Conversely, H-6 is β -oriented and interacts with H-5; these two protons are therefore being in *gauche*-configuration as also supported by the coupling constant ($J = 5, 6: 7.0$ Hz). The seven-member ring is a *quasi*-boat like shape with the concave side pointing towards the β -side of the molecule. This can be seen from the mutual NOE correlations between Me-15 with H-1 and Me-11, H-1, H-2, and H-3 with H₃-4. An interaction through space of the hydroxyl proton (δ 3.06, 1H, *bs*) at C-10 with H-12 (δ 1.14, *m*) and H-4 (δ 3.18, *m* in CDCl₃) is only possible for the α -orientation of the tertiary hydroxyl group on C-10. Other couplings between β -oriented H₃-11 (δ 2.24, *s*) and H-5 (δ 1.96, *ddd*) and H₃-15 (δ 1.17, *d*) also indicated a α -stereochemistry for the hydroxyl substituent. The stereochemistry at the tertiary alcohol was established by the fact that Me-11 has mutual NOE correlations with H-1 and Me-15, which had shown to be in the β -face of the molecule (axial configuration) under observation, and the secondary alcohol group that appeared as a broad singlet (at δ 3.06 ppm) has NOE interactions with H-4 and H-12, as well as H₃-14 and H₃-13 in the molecule. This is only possible if the hydroxyl group lies on the α -side of the molecule. Furthermore, the NOE between H-9 and H-14 and the coupling constant between protons at H-8 and H-9 (1.5 Hz, 4.8 Hz) indicated that the hydroxyl group at C-10 and the cycloheptane ring are in the same plane. Based upon these observations it can be concluded that a hydroxyl function for **1** to guai-2-en-10 α -ol indubitably existed at C-10.

Guai-2-en-10 α -methanol (**2**) was isolated as colorless oil. The IR spectrum revealed prominent absorption band at ν_{\max} 3500 cm⁻¹, attributed to hydroxyl functionality, and to olefinic system (1565, 1620, 1380, 985 cm⁻¹). The MS shown the molecular ion signal at $m/z = 222.3715$, and its molecular formula established as C₁₅H₂₆O based upon the combination of MS, and extensive NMR experiments. The ¹H and ¹³C NMR spectra indicated the presence of three methyl groups (δ_{H} 0.96, *s*; 0.87, *t*; and 1.13, *d*), and one double bond (δ_{H} 5.58, 5.70; *m*) (Table 2). The position of hydroxymethyl group (-CH₂OH) was determined by analyses of ¹H NMR spectrum that shows two singlets at δ 3.54 and δ 3.40 ppm, respectively (Table 2). The ¹³C NMR spectrum exhibited signals for all 15 carbons, including one hydroxymethyl (δ_{C} 70.8); two tertiary vinyl carbons (δ_{C} 132.7 and 135.5 ppm), five methylenes (δ_{C} 33.4, 23.1, 37.2, 28.4, and 70.8 ppm), five methine carbons (δ_{C} 43.8, 132.7, 44.2, 35.8, and 36.7 ppm), and three methyl groups (δ_{C} 11.9, 18.4, and 19.4 ppm) (Table 2). One methylenic signal (-CH₂-) appeared downfield at δ 70.8 apparently due to the presence of an electronegative atom (-O-). With an unsaturation degree of three, the structure was suggested to contain, besides one double bond, two rings. Significant ¹H-¹H COSY correlations are apparent between protons positioned at H-5/H-6/H-7/H-8/H-9, thus confirming cycloheptane ring skeleton [13]. The ¹H-¹H COSY couplings between H-1/H-2, H-4/H-3, 5, and H-3/H-4 supported the presence of cyclopentane ring skeleton (Fig. 4). ¹H-¹H COSY correlations between H-6/H-13/H14 support the presence of ethyl moiety. The HMBC long range correlations between H-7 (δ_{H} 1.09) and H-8 (δ_{H} 1.20) with C-6 (δ_{C} 36.7), and those of H₃-14 (δ_{H} 0.87) with C-4 (δ 44.2), C-5 (δ 35.8), C-6 (δ_{C} 36.7), and C-13 (δ_{C} 11.9) indicated the ethyl side chain to be linked to C-6 (Fig. 4). The correlations between H₃-12/C-10, and between H₃-15/C-4, indicated the positions of the respective methyl groups at C-12 and C-15 positions. The equatorial position of the hydroxymethyl group (-CH₂OH) is confirmed by its mutual NOE correlation with the β -oriented ethyl group (Fig. 5), and not with H-1/H₃-12 or H₃-15/H-5. This suggests that H-1 and H-5 are in *cis*-configuration, and placed at the axial position (β -orientation), whereas the hydroxymethyl group, as well as the ethyl group are located on the β -face of the molecule (axial in configuration). After adding shift reagent (Eu(fod)₃), a pronounced NOE correlation was

Table 2
NMR spectroscopic data of guai-2-en-10 α -methanol (**2**) in CDCl₃.^a

Carbon No.	$\delta^{13}\text{C}$ NMR (DEPT)	H	$\delta^1\text{H}$ NMR (int., mult., <i>J</i> in Hz)	¹ H- ¹ H COSY	HMBC (H-C)
1	45.8 (CH)	-	-	-	-
	-	1 β	2.26 (<i>m</i>)	-	C-1, 5, 10
2	132.7 (CH)	2H	5.70 (<i>m</i>)	-	C-2, 3, 4
	-	-	-	-	-
3	135.5 (CH)	3H	5.58 (<i>m</i>)	H-4	C-3, 4
	-	-	-	-	-
4	44.2 (CH)	4 α	2.86 (<i>dd</i> , <i>J</i> = 7.5, 5.6 Hz)	H-3, 5	C-4, 15
5	35.8 (CH)	5 β	1.88 (<i>ddd</i> , <i>J</i> = 7.0, 6.8, 7.5 Hz)	H-4, 6	C-1, 5
6	36.7 (CH)	-	-	H-5, 7, 13	C-6, 7, 8, 13
	-	6 β	1.75 (<i>d</i> , <i>J</i> = 7.0 Hz)	-	-
7	33.4 (CH ₂)	7 α	1.09 (<i>t</i> , <i>J</i> = 6.2, 7.4 Hz)	H-6, 8	C-7, 8
	-	7 β	1.18 (<i>m</i>)	-	-
8	23.1 (CH ₂)	8 α	1.20 (<i>m</i>)	H-7, 9	C-7, 8, 9
	-	8 β	1.26 (<i>t</i> , <i>J</i> = 5.6, 6.3 Hz)	-	-
9	37.2 (CH ₂)	9 α	1.05 (<i>t</i> , <i>J</i> = 5.2, 3.9 Hz)	H-8	C-8, 10
	-	9 β	1.30 (<i>d</i> , <i>J</i> = 3.8 Hz)	-	-
10	35.3 (C)	-	-	-	C-9, 11, 12
11	70.8 (CH ₂)	11 α	3.40 (<i>s</i>)	-	C-1, 10, 12
	-	11 β	3.54 (<i>s</i>)	-	-
12	19.4 (CH ₃)	CH ₃ -12	0.96 (<i>s</i>)	-	C-10, 11
13	28.4 (CH ₂)	13 α	1.22 (<i>m</i>)	H-6, 14	C-6, 14
	-	13 β	1.33 (<i>d</i> , <i>J</i> = 6.5 Hz)	-	-
14	11.9 (CH ₃)	CH ₃ -14	0.87 (<i>t</i> , <i>J</i> = 6.3 Hz)	H-13	C-4, 5, 6, 13
15	18.1 (CH ₃)	CH ₃ -15	1.13 (<i>d</i> , <i>J</i> = 6.5 Hz)	H-4	C-4

^a The notations are as indicated under Table 1.

observed between H-4 and H-11 as well as with H-13 protons thus suggesting them on the same face (α -orientation) of the molecule. A pronounced NOESY correlation between H₃-15 with H₃-11 consistent with their *cis*-orientation on the top face (β) of the molecule. Pronounced NOE correlations also were apparent between H β -8 with H₃-15, which in turn was found to be correlated with H β -1, H β -5, and CH₃-11. These results confirm the *cis*-orientation at the top face (axial orientation) of the molecule. Pronounced NOE correlations are observed between C-4 bearing -CH₃ group (CH₃-15) with H-1 and H-5 ring junction carbon, thus suggesting the methyl group located at the β -face of the molecule. Significant NOE interactions between ethyl group and hydroxymethyl protons suggested them at α -face of the molecule with equatorial orientation (Fig. 5).

The molecular formula of guai-2-en-10 α -methyl methanoate (**3**) as C₁₇H₂₈O₂ was determined by the analysis of MS and extensive NMR spectroscopic data. The presence of a carbonyl was

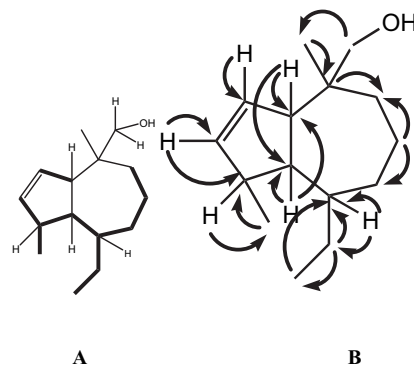


Fig. 4. 2D NMR couplings observed in guai-2-en-10 α -methanol (**2**). A: Key ¹H-¹H COSY couplings (bold face bonds); B: HMBC correlation (C-H couplings are indicated as double barbed arrow).

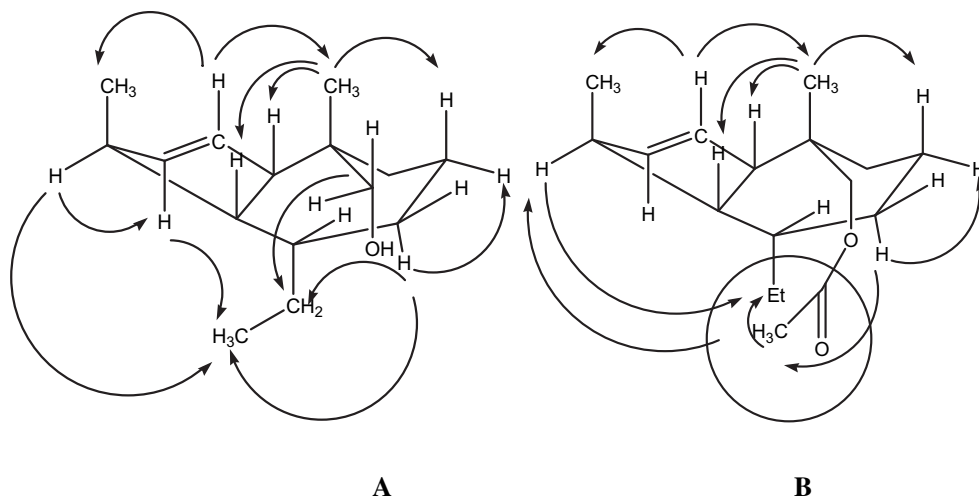


Fig. 5. Key NOESY correlations of **2** and **3**. The hydroxyl group in **2** is equatorial resulting in long range coupling of β -H at C-3 with CH_3 at 6th carbon of the alicyclic ring. In **3**, the axially oriented α -H atom was found to exhibit NOE couplings with C-3 hydrogen and side chain protons.

established by IR spectrometry (1720 cm^{-1}) and ^{13}C NMR spectrum (δ_{C} 176.3) (Table 3). The ^1H NMR spectrum displayed the signals of four methyls at CH_3 -12, 14, 15, and carboxymethyl group ($-\text{COCH}_3$) as appeared at δ 1.12 (s), 0.93 (t), 1.19 (d), and 2.06 (s), respectively. The ^1H NMR spectra of **2** and **3** showed very similar signals except for the change of primary acetate ($-\text{COCH}_3$) to a hydroxymethyl group ($-\text{CH}_2\text{OH}$) (Table 3). Moreover, analysis of the spectra suggested a sesquiterpenoid nature, and the easy chemical interconversion of **3** into **2** and vice-versa, caused by hydrolysis and acetylation respectively, indicated that **3** was the monoacetyl derivative of **2**.

Guai-2-en-10 α -methyl methanoate (**3**) exhibited significant activity against *Vibrio parahaemolyticus* ATCC 17809 (MIC: 25 $\mu\text{g}/\text{mL}$). Guai-2-en-10 α -methanol (**2**) has lower activity (zone size: 13.20 mm against the bacterium with 150 μg loading; MIC: 35 $\mu\text{g}/\text{mL}$) as compared to that of guai-2-en-10 α -methyl methanoate (**3**) apparently due to the presence of more polarisable (polarisability $7.02 \times 10^{-24}\text{ cm}^3$) C-10 acetyl group as compared to the less polarisable hydroxymethyl group ($3.25 \times 10^{-24}\text{ cm}^3$) in guai-2-en-10 α -methanol (**2**) (Table 4). The electronic effects rather than bulk parameters (parachor) have a significant influence on the bioactivity. The direct involvement of polarisability (PI) with the target bioactivity in the guaiene sesquiterpenoids implied that inductive (field/polar) rather than steric effect (parachor) of the side chain at C-10 appears to be the key factor influencing the induction of antibacterial activity (Fig. 6). Guai-2-en-10 α -methyl methanoate (**3**) was found to be highly active against *Vibrio parahaemolyticus* ATCC 17809 and *V. vulnificus* MTCC 1146 (MIC: 25 $\mu\text{g}/\text{mL}$) than guai-2-en-10 α -methanol (**2**) (zone sizes: 13.20 and 12.90 mm against *Vibrio parahaemolyticus* ATCC 17809 and *V. harveyi* MTCC 3438, with 150 μg loading) because methyl methanoate moiety in ((1R, 4S)-4-ethyl-1-methyl-cycloheptyl)methyl acetate (polarisability $24.56 \times 10^{-24}\text{ cm}^3$) fragment has a very high polarisability value (polarisability $7.02 \times 10^{-24}\text{ cm}^3$) as compared to ((1R,4S)-4-ethyl-1-methyl-cycloheptyl)methanol (devoid of acetyl group) with comparatively lower field effect (polarisability $20.79 \times 10^{-24}\text{ cm}^3$). It can be inferred that guai-2-en-10 α -methyl methanoate (**3**) with highly electronegative acetyl group withdraw the electron cloud by a combination of inductive ($-I$ effect) and mesomeric effect ($+M$ -effect) from the substituted cycloheptyl ring as well as (R)-3-methylcyclohept-1-ene moiety of guai-2-en-10 α -methyl methanoate (**3**), thus acting as the nucleophilic center of the molecule resulting in a high level of activity (Fig. 6). Guai-2-en-10 α -ol (**1**) with (1R, 4S)-4-ethyl-1-methyl-

cycloheptanol moiety exhibited lowest activity against *Vibrio parahaemolyticus* ATCC 17809 (MIC: 110 $\mu\text{g}/\text{mL}$) and *V. harveyi* MTCC 3438 (MIC: 160 $\mu\text{g}/\text{mL}$) apparently due to lower polarisability value ($20.75 \times 10^{-24}\text{ cm}^3$). These leads will be significant in explaining the pharmacophore-fit in the macromolecular receptor site and exploring the primary site and mode of action of this class of guaiene sesquiterpenoids.

Table 3
NMR spectroscopic data of guai-2-en-10 α -methyl methanoate (**3**) in CDCl_3 .^a

Carbon No.	$\delta^{13}\text{C}$ NMR (DEPT)	H	$\delta^1\text{H}$ NMR (int., mult., J in Hz)	$^1\text{H}-^1\text{H}$ COSY	HMBC (H-C)
1	45.4 (CH)	–	–	–	–
2	132.9 (CH)	1 β	2.29 (m)	–	C-1, 10
		2H	5.76 (m)	–	C-2, 3, 4
3	143.1 (CH)	3H	5.63 (m)	H-4	C-3, 4
		–	–	–	–
4	44.3 (CH)	4 α	2.73 (dd, J = 6.3, 5.6 Hz)	H-5	C-4
		–	–	–	–
5	36.2 (CH)	5 β	1.79 (ddd, J = 7.0, 6.5, 7.5 Hz)	H-4, 6	C-1, 5
		–	–	–	–
6	36.8 (CH)	–	–	H-5, 7, 13	C-6, 7, 8, 13
		–	–	–	–
7	34.1 (CH ₂)	6 β	1.68 (d, J = 7.0 Hz)	–	–
		7 α	1.09 (t, J = 5.8, 7.0 Hz)	H-6, 8	C-7, 8
8	22.8 (CH ₂)	7 β	1.25 (m)	–	–
		8 α	1.16 (m)	H-7	C-8, 9
9	37.5 (CH ₂)	8 β	1.28 (t, J = 4.8, 5.5 Hz)	–	–
		9 α	1.05 (t, J = 5.5, 3.8 Hz)	H-8	C-8, 10
10	41.5 (C)	9 β	1.32 (m)	–	–
		–	–	–	–
11	73.8 (CH ₂)	11 α	3.65 (s)	–	C-1, 6, 10, 12
		11 β	3.80 (s)	–	–
12	20.6 (CH ₃)	CH ₃ -12	1.12 (s)	–	C-10, 11
13	27.4 (CH ₂)	13 α	1.25 (m)	H-14	C-6, 14
		13 β	1.31 (d, J = 6.0 Hz)	–	–
14	11.6 (CH ₃)	CH ₃ -14	0.93 (t, J = 6.5 Hz)	H-13	C-4, 5, 6, 13
		–	–	–	–
15	20.1 (CH ₃)	CH ₃ -15	1.19 (d, J = 5.8 Hz)	H-4	C-4
	176.3 (C=O)	–	3.90 (m)	–	–
	20.5 (–COCH ₃)	CH ₃ acetyl	2.06(s)	–	–

^a The notations are as indicated under Table 1.

Table 4
In vitro antibacterial activity of guanolides (1–3) on three *Vibrio* sp.

Co. No. ^a	<i>Vibrio parahaemolyticus</i> ATCC 17809				<i>V. harveyi</i> MTCC 3438				<i>V. vulnificus</i> MTCC 1146			
	IZD (mm) ^b			MIC (µg/mL)	IZD (mm) ^b			MIC (µg/mL)	IZD (mm) ^b			MIC (µg/mL)
	50 µg	100 µg	150 µg		50 µg	100 µg	150 µg		50 µg	100 µg	150 µg	
1	6.83c	6.92b	7.28a	110	6.54c	6.58c	6.60c	160	7.15a	7.30a	7.85a	125
2	12.68b	12.90a	13.20a	35	10.58b	11.65b	12.90b	50	11.70b	12.00a	12.40a	40
3	15.29a	15.85a	16.65a	25	11.73b	12.34b	12.59b	30	14.10a	14.93a	15.08a	25

^a Co. No. indicates compound number.

^b IZD implies inhibition zone diameter expressed as mm, inhibition zone diameters are indicated at three different loadings 50, 100, and 150 µg of test compounds; Results are expressed as inhibition of bacterial growth (inhibition zone diameter in mm) and MIC (µg/mL) as determined by broth microdilution assay at different concentrations of test compounds (10–250 µg/mL). Different alphabets (a–c) indicate significant difference among different treatments (Tukey's multiple range test).

3. Experimental

3.1. General experimental procedures

Fourier-transform infrared (FTIR) spectra of KBr pellets were recorded in a Perkin–Elmer Series 2000 FTIR spectrophotometer scanning between 4000 and 400 cm^{-1} . ^1H and ^{13}C NMR spectra were recorded on a Bruker Avance DPX 300 (300 MHz) spectrometer in CDCl_3 or $\text{DMSO}-d_6$ as aprotic solvent at ambient temperature with TMS as the internal standard ($\delta = 0$ ppm). Standard pulse sequences were used for DEPT, $^1\text{H}-^1\text{H}$ COSY, two-dimensional NOESY, HMQC, and HMBC experiments. The GC analyses were accomplished on a Perkin Elmer Gas chromatograph equipped with an Elite – 5 capillary column (30 m \times 0.53 mm i.d.) using a flame ionization detector (FID) equipped with a split/splitless injector, which was used in the split (1:15) mode. The oven temperature ramp program: 60 °C for 10 min, rising at 5 °C/min to 220 °C; injector and detector temperatures 250 °C; carrier gas, nitrogen (ultra high purity >99.99%, 3 mL/min). The injection port temperature was maintained at 285 °C. The GC–MS analyses were performed in electronic impact (EI) ionization mode in a Varian GC (CP-3800) interfaced with a Varian 1200L single quadrupole Mass Spectrometer for confirmation of the fatty acids identification. The GC apparatus was equipped with WCOT fused silica capillary column of high polarity (DB-5; 30 m \times 0.25 mm i.d.). The carrier gas was ultra high purity

He. The injector (type 1079) and detector temperatures were maintained isothermal at 300 °C. Samples (1 µL) were injected in split (1:15) mode at 300 °C into the capillary column similar to that used for the GC analyses, and the oven was identically programmed. Ion source and transfer line were kept at 300 °C. All compounds were of analytical, spectroscopic or chromatographic reagent grade, and were obtained from E-Merck (Darmstadt, Germany). All reagents and chemical solvents used for products isolation were of analytical grade or higher. The microbial strains, *Vibrio harveyi* MTCC 3438, and *Vibrio vulnificus* MTCC 1146 have been procured from Microbial Type Culture Collection Centre of Institute of Microbial Technology, Chandigarh, India, whereas *Vibrio parahaemolyticus* ATCC 17809 has been procured from HiMedia.

3.2. Algal material and preparation of crude extracts

The seaweed samples of *Ulva fasciata* were harvested in December 2003 from an exposed intertidal rocky shore in Vizhinjam and Mullur (Kerala State, India). Voucher specimens have been deposited in the Vizhinjam Research Centre of CMFRI. The air-dried sample of *U. fasciata* was cold extracted with cold CH_3OH for 1 week. The MeOH extract was filtered, and the aliquot has been concentrated *in vacuo* at a temperature below 45 °C to afford a crude extract (56 g), which was partitioned between $\text{CHCl}_3/\text{MeOH}$ (1:1, v/v) to furnish viscous brown oil (13.8 g).

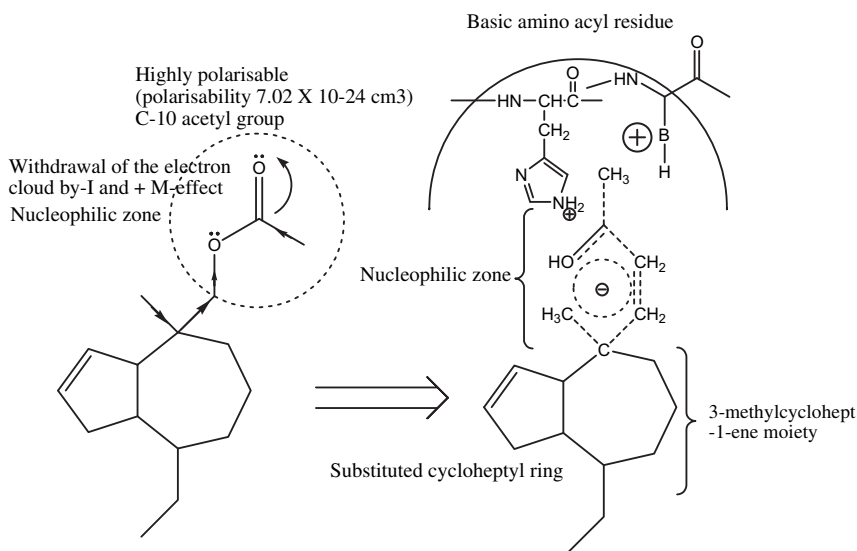


Fig. 6. Sketch model of guai-2-en-10 α -methyl methanoate (3). Induction of bioactivity is directly proportional to the inductive (field/polar effect) and resonance effects of the methyl methanoate moiety. Guai-2-en-10 α -methyl methanoate with highly electronegative acetyl group withdraw the electron cloud by a combination of inductive (-I effect) and mesomeric effect (+M-effect) from the substituted cycloheptyl ring as well as (R)-3-methylcyclohept-1-ene moiety of guai-2-en-10 α -methyl methanoate, thus acting as the nucleophilic center of the molecule resulting in a high level of activity.

3.3. Chromatographic purification of guaiane sesquiterpenoides from *U. fasciata*

The resulting crude $\text{CHCl}_3/\text{MeOH}$ extract (3.0 g) was fractionated by chromatography over neutral alumina (70–230 mesh), with a stepwise gradient of *n*-hexane/ CH_2Cl_2 (9.5:0.5 to 1:1, v/v) to provide ten fractions (50 mL, F_1 – F_{10}). Fraction F_7 as eluted by *n*-hexane/ CH_2Cl_2 (3:7, v/v) was fractionated with *n*-hexane/EtOAc (98:2, 92:8, 85:15, 80:20, and 75:25, v/v) to give 40 subfractions (SF_1 – SF_{40}). The fractions SF_{15} – SF_{20} were further applied to an alumina column to give a mixture, which was further fractionated with $\text{CH}_2\text{Cl}_2/\text{EtOAc}$ (95:5, 85:15, 75:25, 70:30, v/v) to give 20 subfractions (SV_1 – SV_{20}). Subfractions SV_{16} – SV_{19} as eluted with $\text{CH}_2\text{Cl}_2/\text{EtOAc}$ (7:3, v/v) were pooled to afford pure guai-2-en-10 α -ol (1, 18.4 mg). The subfraction SV_5 was further separated by chromatography on alumina coated with AgNO_3 using a stepwise gradient system from *n*-hexane/EtOAc (9:1, 8:2, 7:3, 6:4, 1:1, 5:6, and 4:7, v/v). Guai-2-en-10 α -methanol (**2**, 24.6 mg) was obtained by eluting with *n*-hexane/EtOAc (5:6, v/v). Evaporation of solvents from the fractions followed by TLC over Si gel GF₂₅₄ (particle size 15 μm) using *n*-hexane/EtOAc (90:10, v/v) supported the purity. Compound **2** (10.0 mg) was acetylated with acetic anhydride (0.5 mL) and pyridine (0.5 mL) at room temperature overnight for 24 h [14]. The product was purified by neutral alumina column chromatography (2.0 \times 20 cm) by using $\text{CH}_2\text{Cl}_2/\text{EtOAc}$ (8:2, v/v), affording the pure monoacetate of **2** (guai-2-en-10 α -methyl methanoate, **3**) (13.6 mg).

3.3.1. Guai-2-en-10 α -ol (**1**)

Yellowish oil; TLC (Si gel GF₂₅₄ 15 μm ; *n*-hexane/EtOAc 90:10, v/v) R_f : 0.45; GC (Elite – 5 capillary column 30 m \times 0.53 mm i.d.; oven temperature ramp: 60 °C for 10 min, rising at 5 °C/min to 220 °C; 1 μL injection volume/ CHCl_3) R_t : 8.35 min.; Elemental analysis found: C, 81.45; H, 11.87; O, 7.21 ($\text{C}_{15}\text{H}_{26}\text{O}$ requires C, 81.02; H, 11.79; O, 7.20); IR ν_{max} (KBr): 3040 (–OH str.), 2962 (methyl –CH str.), 1461, 1035, 820 cm^{-1} (olefinic moiety); ^1H (CDCl_3 , 300 MHz, δ ppm) and ^{13}C NMR (CDCl_3 , δ ppm) data, see Table 1; EIMS m/z (rel. int.%) 222 [$\text{M}]^+$ (18), 208 (19), 205 (10), 180 (36), 178 (11), 122 (6), 124 (56), 126 (6), 122 (100), 96 (79), 56 (95); HRMS (ESI): calcd. for $\text{C}_{15}\text{H}_{26}\text{O}$ 222.3694; found 222.3719 [$\text{M} + \text{H}]^+$.

3.3.2. Guai-2-en-10 α -methanol (**2**)

Colorless oil; TLC (Si gel GF₂₅₄ 15 μm ; *n*-hexane/EtOAc 90:10, v/v) R_f : 0.42; GC (Elite – 5 capillary column 30 m \times 0.53 mm i.d.; oven temperature ramp: 60 °C for 10 min, rising at 5 °C/min to 220 °C; 1 μL injection volume/ CHCl_3) R_t : 8.40 min.; Elemental analysis found: C, 81.21; H, 11.86; O, 7.23 ($\text{C}_{15}\text{H}_{26}\text{O}$ requires C, 81.02; H, 11.79; O, 7.20); IR ν_{max} (KBr): 3450 (–OH str.), 3282 (as. sec. –OH str.), 2842 (methyl CH str.), 1589, 1430, 842 cm^{-1} (olefinic moiety); ^1H (CDCl_3 , 300 MHz, δ ppm) and ^{13}C NMR (CDCl_3 , δ ppm) data, see Table 2; EIMS m/z (rel. int.%) 222 [$\text{M}]^+$ (16), 194 (66), 178 (9), 180 (22), 124 (65), 122 (100), 96 (80), 56 (29); HRMS (ESI): calcd. for $\text{C}_{15}\text{H}_{26}\text{O}$ 222.3694; found 222.3715 [$\text{M} + \text{H}]^+$.

3.3.3. Guai-2-en-10 α -methyl methanoate (**3**)

Colorless oil; TLC (Si gel GF₂₅₄ 15 μm ; *n*-hexane/EtOAc 90:10, v/v) R_f : 0.39; GC (Elite – 5 capillary column 30 m \times 0.53 mm i.d.; oven temperature ramp: 60 °C for 10 min, rising at 5 °C/min to 220 °C; 1 μL injection volume/ CHCl_3) R_t : 11.25 min.; Elemental analysis found: C, 77.41; H, 10.75; O, 12.12 ($\text{C}_{17}\text{H}_{28}\text{O}_2$ requires C, 77.22; H, 10.67; O, 12.10); IR ν_{max} (KBr): 3500, 2839 (methyl –CH str.), 1745 (C=O str.), 1735 (amide-II band), 1365, 1192, 1010, 830 cm^{-1} (olefinic moiety); ^1H (CDCl_3 , 300 MHz, δ ppm) and ^{13}C NMR (CDCl_3 , δ ppm) data, see Table 3; EIMS m/z (rel. int.%) 264 [$\text{M}]^+$ (12), 224 (26), 225 (8), 210 (31), 208 (32), 179 (18), 124 (14), 122 (100), 126 (6), 96 (81), 56 (92); HRMS (ESI): calcd. for $\text{C}_{17}\text{H}_{28}\text{O}_2$ 264.4062; found 264.4084 [$\text{M} + \text{H}]^+$.

3.4. Antibacterial activity of the guaianolides and structure-activity correlation analyses

The *in vitro* antibacterial activities of the biomolecules against test vibrios were tested by the disc-diffusion method [15,16], and minimum inhibitory concentration (MIC) as determined by microdilution method [17]. For susceptibility testing, all the stock solutions of the fractions have been prepared in Me_2SO , except for *n*-hexanic fractions, which were dissolved in CH_3OH . For agar disc-diffusion assay, Zobell agar (10 mL) was introduced into sterile petri dishes (9 cm diameter), and inoculated with 1 mL of 18 h 15% NaCl TSA broth culture (10^7 bact./mL). Blank paper discs (6 mm diameter, sterile blank) were impregnated with Me_2SO as negative controls, and discs of chloramphenicol and ampicillin as positive controls, with test compounds (50, 100, and 150 μg loading), which were placed on petri plates containing Mueller Hinton agar impregnated with bacterial suspensions. The plates were incubated overnight at 37 °C and the antibacterial activity was defined as the diameter (in mm) of the clear inhibitory zone formed around the paper disc. To determine the MIC of the test compounds (0.5 mg) were diluted in Me_2SO (500 μL) and mixed with bacterial strains cultured in nutrient broths (9.5 mL). The initial concentration of test compounds was 4 mg/mL, and concentrations of 10, 20, 30, 40, 50, 60, 70, 80, 90, 100, 150, 200, and 250 $\mu\text{g}/\text{mL}$ were obtained by serial dilutions. Antibacterial test was performed by transferring 10 mL of each bioassay culture (bacterial culture with test compounds) into a new test tube containing only nutrient broth. Observations were made after 24 h to determine possible bacterial growth in the respective culture broths. Optical density of treated cells reflects their viability and provides sufficient information pertaining to the mode of action of the tested metabolites. Structure-activity correlation analyses were applied to the guaionolide sesquiterpenoids by using the electronic and bulk parameters. Parachor was chosen as the bulk descriptor, whereas polarisability was taken as electronic descriptor variable [18–20].

3.5. Statistical analysis

Results of the bacterial counts were analyzed using the one-way analysis of variance (ANOVA) following the statistical program for the social sciences (SPSS, ver. 13.0). A significance level of 95% ($p = 0.05$) was used throughout, and significant difference among different treatments was determined by Tukey's multiple range test. All measurements were performed in triplicate ($n = 3$), and values were averaged.

Acknowledgements

The authors are thankful to the Director, CMFRI, Cochin for providing necessary facilities to carry out the work. Thanks are also due to Dr. S. Saravanan, Doctoral fellow of Madurai Kamaraj University for recording NMR spectra.

References

- [1] J. Kubanek, P. Jensen, P.A. Keifer, M.C. Sullards, D.O. Collins, W. Fencial, Proc. Natl. Acad. Sci. U.S.A. 100 (2003) 6916–6921.
- [2] D.J. Faulkner, Nat. Prod. Rep. 19 (2002) 1–48.
- [3] J.W. Blunt, B.R. Copp, M.H.G. Munro, P.T. Northcote, M.R. Prinsep, Nat. Prod. Rep. 23 (2006) 26–78.
- [4] J.T. Handley, A.J. Blackman, Aust. J. Chem. 58 (2005) 39–46.
- [5] M.P. Puglisi, L.T. Tan, P.R. Jensen, W. Fenical, Tetrahedron 60 (2004) 7035–7039.
- [6] A.S.R. Anjaneyulu, C.V.S. Prakash, U.V. Mallavadhani, Phytochemistry 30 (1991) 3041–3042.
- [7] F.E. Koehn, S.P. Gunasekera, D.N. Neil, S.S. Cross, Tetrahedron Lett. 32 (1991) 169–172.
- [8] V.J. Paul, J.M. Cronan Jr., J.H. Cardellina II, J. Chem. Ecol. 19 (1993) 1847–1860.

- [9] F. Frohloff, L. Fichtner, D. Jablonowski, K.D. Breunig, R. Schaffrath, *EMBO J.* 20 (2001) 1993–2003.
- [10] D.J. Alderman, T.S. Hastings, *Int. J. Food Sci. Technol.* 33 (1998) 139–155.
- [11] R. Selvin, A.J. Huxley, A.P. Lipton, *Aquaculture* 230 (2004) 241–248.
- [12] J.A. Faraldos, S. Wu, J. Chappell, R.M. Coates, *Tetrahedron* 63 (2007) 7733–7742.
- [13] T. Hackl, W.A. Konig, H. Muhle, *Phytochemistry* 65 (2004) 2261–2275.
- [14] L. Zaiter, M. Bouheroum, S. Benayache, F. Benayache, F. León, I. Brouard, J. Quintana, F. Estévez, J. Bermejo, *Biochem. Syst. Ecol.* 35 (2007) 533–538.
- [15] A.W. Bauer, W.M.M. Kirby, J.C. Scherris, M. Turck, *Am. J. Clin. Pathol.* 45 (1966) 493–496.
- [16] L.A. Mitscher, R.P. Leu, M.S. Bathala, W.N. Wu, J.L. Beal, R. White, *Lloydia* 35 (1972) 157–166.
- [17] R.N. Jones, A.L. Barry, *J. Antimicrob. Chemother.* 19 (1987) 841–842.
- [18] K. Chakraborty, C. Devakumar, *J. Agric. Food Chem.* 53 (2005) 3468–3475.
- [19] K. Chakraborty, C. Devakumar, *J. Agric. Food Chem.* 54 (2006) 1868–1873.
- [20] K. Chakraborty, C. Devakumar, S.M.S. Tomar, R. Kumar, *J. Agric. Food Chem.* 51 (2003) 992–998.